

Metal-insulator transition and the Pr³⁺/Pr⁴⁺ valence shift in (Pr_{1-y}Y_y)_{0.7}Ca_{0.3}CoO₃J. Hejtmánek, E. Šantavá, K. Knížek, M. Maryško, and Z. Jirák
Institute of Physics, ASCR, Cukrovarnická 10, 162 00 Prague 6, Czech Republic

T. Naito, H. Sasaki, and H. Fujishiro

Faculty of Engineering, Iwate University, 4-3-5 Ueda, Morioka 020-8551, Japan

(Received 23 April 2010; revised manuscript received 22 July 2010; published 5 October 2010)

The magnetic, electric, and thermal properties of the $(Ln_{1-y}Y_y)_{0.7}Ca_{0.3}CoO_3$ perovskites ($Ln=Pr,Nd$) were investigated down to very low temperatures. The main attention was given to a peculiar metal-insulator (M-I) transition, which is observed in the praseodymium based samples with $y=0.075$ and 0.15 at $T_{M-I}=64$ K and 132 K, respectively. The study suggests that the transition, reported originally in $Pr_{0.5}Ca_{0.5}CoO_3$, is not due to a mere change in cobalt ions from the intermediate to the low-spin states but is associated also with a significant electron transfer between Pr^{3+} and Co^{3+}/Co^{4+} sites, so that the praseodymium ions occur below T_{M-I} in a mixed Pr^{3+}/Pr^{4+} valence. The presence of Pr^{4+} ions in the insulating phase of the yttrium doped samples $(Pr_{1-y}Y_y)_{0.7}Ca_{0.3}CoO_3$ is evidenced by Schottky peak originating in Zeeman splitting of the ground-state Kramers doublet. The peak is absent in pure $Pr_{0.7}Ca_{0.3}CoO_3$ in which metallic phase, based solely on non-Kramers Pr^{3+} ions, is retained down to the lowest temperature.

DOI: [10.1103/PhysRevB.82.165107](https://doi.org/10.1103/PhysRevB.82.165107)

PACS number(s): 71.30.+h, 65.40.Ba

I. INTRODUCTION

Thermally induced transitions in $LnCoO_3$ ($Ln=La, Y$, rare earths) have been studied for decades. Recent interpretation associates them with a local excitation of the octahedrally coordinated Co^{3+} ions from LS (low spin, t_{2g}^6) to HS (high spin, $t_{2g}^4e_g^2$) state, followed at higher temperature by a formation of a metallic phase of IS character (intermediate spin, $t_{2g}^5\sigma^*$)—see, e.g., Ref. 1 and citations therein. An attention is attracted also to the mixed-valence cobaltites such as $La_{1-x}Sr_xCoO_3$ or $La_{1-x}Ca_xCoO_3$ where a similar transition from insulating LS Co^{3+} ground state toward the metallic $t_{2g}^5\sigma^*$ one is obtained in the course of doping ($0 < x < 0.2$). As concerns the metallic region beyond $x=0.2$, some heavily doped Pr-based cobaltites, in particular $Pr_{0.5}Ca_{0.5}CoO_3$ behave anomalously. At ambient temperature, they appear in the metallic $t_{2g}^5\sigma^*$ phase as expected but on cooling they undergo a sharp metal-insulator (M-I) transition at $T_{M-I}=90$ K, documented for the first time by Tsubouchi *et al.*^{2,3} The same transition was observed also on the less-doped samples $Pr_{1-x}Ca_xCoO_3$ ($x=0.3$) under high pressures or upon a partial substitution of praseodymium by smaller rare earth cations or yttrium.⁴⁻⁶ The effect was tentatively ascribed to a change in the cobalt states from itinerant ones $t_{2g}^5\sigma^*$ to a mixture of localized LS $Co^{3+}(t_{2g}^6, S=0)$ and LS $Co^{4+}(t_{2g}^5, S=1/2)$ states. Very recently, an alternative explanation has been proposed based on electronic-structure calculations and some indirect experimental data, namely, the significant lattice contraction and shortening of Pr-O bond lengths that accompany the M-I transition.^{7,8} It is suggested that the formal cobalt valency in $Pr_{0.5}Ca_{0.5}CoO_3$ is changed at T_{M-I} from the mixed-valence $Co^{3.5+}$ toward pure Co^{3+} with strong preference for LS state, and the praseodymium valence is simultaneously increased from Pr^{3+} toward Pr^{4+} . The spin-state transition and formation of an insulating state in $Pr_{0.5}Ca_{0.5}CoO_3$ is thus an analogy of the compositional transition from ferromagnetic (FM) metal

 $La_{0.5}Sr_{0.5}CoO_3$ to diamagnetic insulator $LaCoO_3$,^{9,10}

The present work concerns the system $(Pr_{1-y}Y_y)_{0.7}Ca_{0.3}CoO_3$ ($y=0-0.15$), which is advantageous with respect to an easier preparation of oxygen stoichiometric samples as compared with the $Pr_{0.5}Ca_{0.5}CoO_3$ system. The M-I transition observed for $y \geq 0.075$ ($T_{M-I}=60-130$ K) is manifested by pronounced anomalies in the temperature course of transport, magnetic, and thermal properties. Fundamental information on the nature of the insulating phase is obtained at very low temperatures. This refers especially to the occurrence of a Schottky peak in the specific heat, centered at 1–2 K. A comparison with the specific-heat data in $Nd_{0.7}Ca_{0.3}CoO_3$ where similar Schottky peak is currently also observed, allows us to conclude that the peak arises due to an exchange field splitting of the doublet ground state of Kramers rare-earth ions, in particular Nd^{3+} . Its occurrence in the yttrium-doped $(Pr_{1-y}Y_y)_{0.7}Ca_{0.3}CoO_3$ provides a direct and quantitative evidence for the fact that in the insulating phase, in addition to common Pr^{3+} (non-Kramers ion), there is a significant significant population of Pr^{4+} (Kramers ion).

II. EXPERIMENTAL

Polycrystalline samples of $(Ln_{1-y}Y_y)_{0.7}Ca_{0.3}CoO_3$ ($Ln=Pr,Nd$) were prepared by a solid-state reaction. Raw powders of Pr_6O_{11} , Nd_2O_3 , Y_2O_3 , Co_3O_4 , and $CaCO_3$ were weighted with proper molar ratios and ground using an agate mortar and pestle for 1 h. Mixed powders were calcined at 1000 °C for 24 h in air. Then they were pulverized, ground, and pressed into pellets of 20 mm diameter and 4 mm thickness. Pellets were sintered at 1200 °C for 24 h in 0.1 MPa flowing oxygen gas. The measured densities of each sample were greater than 90% of the ideal density. Powder x-ray diffraction patterns were taken for each sample using $Cu K\alpha$ radiation; the samples were confirmed to have a single phase orthorhombite ($Pbnm$) structure.

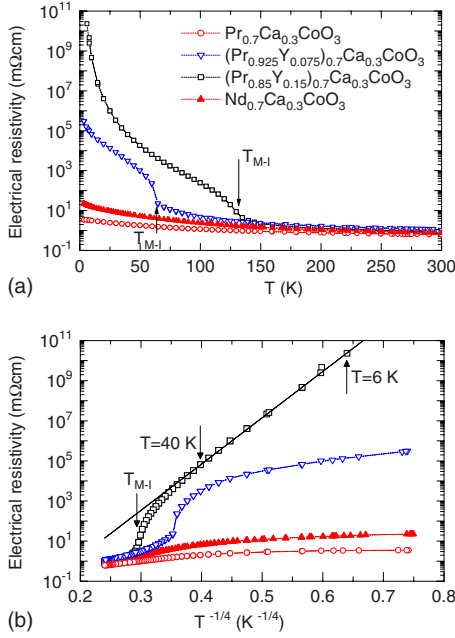


FIG. 1. (Color online) The temperature dependence of electrical resistivity in $(\text{Pr}_{1-y}\text{Y}_y)_{0.7}\text{Ca}_{0.3}\text{CoO}_3$ ($y=0, 0.075$, and 0.15) and $\text{Nd}_{0.7}\text{Ca}_{0.3}\text{CoO}_3$. The data measured on cooling and warming are overlapping. The lower panel shows the dependence on $T^{-1/4}$.

The magnetic measurements were performed in the temperature range from 2 to 400 K using a superconducting quantum interference device magnetometer Magnetic Property Measuring System device (Quantum Design). The hysteresis loops at $T=2$ and 4.5 K were recorded between the field -7 and 7 T. The susceptibility was measured under an applied field of 0.1 T, employing the zero-field and field-cooled regimes during warming and cooling the sample, respectively.

Thermal conductivity, thermoelectric power and electrical resistivity were measured using a four-probe method with a parallelepiped sample cut from the sintered pellet. The electrical current density varied depending on the sample resistivity between 10^{-1} A/cm² (metallic state) and 10^{-7} A/cm² (insulating state). The measurements were done on sample cooling and warming using a close-cycle cryostat working down to 2–3 K. The detailed description of the cell including calibration is described elsewhere.¹¹

The specific heat was measured by Physical Property Measuring System device (Quantum Design) using the two- τ model. The data were collected generally on sample cooling. The experiments at very low temperatures (down to 0.4 K) were done using the He³ option.

III. RESULTS

A. Physical characterization

The electric transport measurements on the $(\text{Pr}_{1-y}\text{Y}_y)_{0.7}\text{Ca}_{0.3}\text{CoO}_3$ samples for $y=0, 0.075$, and 0.15 and on $\text{Nd}_{0.7}\text{Ca}_{0.3}\text{CoO}_3$ are presented in Figs. 1 and 2. It is seen that the $y=0$ and analogous neodymium sample are metallic over the whole temperature range, tending to a finite resis-

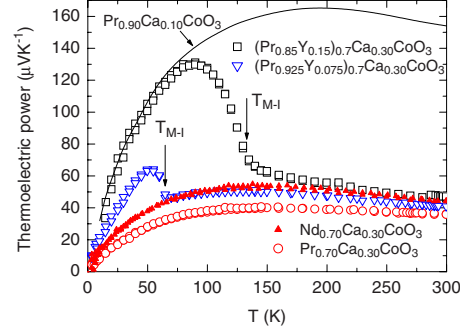


FIG. 2. (Color online) The enhanced Seebeck coefficient in $(\text{Pr}_{1-y}\text{Y}_y)_{0.7}\text{Ca}_{0.3}\text{CoO}_3$ ($y=0.075$ and 0.15) below the M-I transition. The data for metallic $\text{Pr}_{0.7}\text{Ca}_{0.3}\text{CoO}_3$ and $\text{Nd}_{0.7}\text{Ca}_{0.3}\text{CoO}_3$ are also shown. The solid line gives data for $\text{Pr}_{0.9}\text{Ca}_{0.1}\text{CoO}_3$ taken of Ref. 13 (see the text).

tivity of about 1 mΩ cm at 0 K. The yttrium doped samples, apparently in the same metallic state at room temperature, exhibit a sudden increase in the electrical resistivity and thermopower (Seebeck coefficient) at $T_{M-I}=64$ K and 132 K for $y=0.075$ and $y=0.15$, respectively. Concurrently, the thermal conductivity exhibits a kink, followed with a recovery at lower temperatures (Fig. 3). The magnetic susceptibility drops markedly (Fig. 4), which is a strong signature that cobalt ions transform to LS states at T_{M-I} . The M-I transition in $(\text{Pr}_{1-y}\text{Y}_y)_{0.7}\text{Ca}_{0.3}\text{CoO}_3$ is further manifested by a pronounced peak in the specific-heat data (Fig. 5). The peak is very narrow $\sim 1-2$ K for $y=0.075$ with lower T_{M-I} , suggesting a first-order character of the transition while it is much broader ~ 15 K for $y=0.15$ with higher T_{M-I} . It is seen also that the values of specific heat below the M-I transition are small compared to $\text{Pr}_{0.7}\text{Ca}_{0.3}\text{CoO}_3$ retaining the metallic phase, which is indicative of a significant change in lattice dynamics in the low-temperature phase of yttrium-doped samples.

The anomalies in the transport, magnetic and thermal data, similar to those in Figs. 1–5, were observed earlier for the prototypical compound $\text{Pr}_{0.5}\text{Ca}_{0.5}\text{CoO}_3$ (Refs. 2 and 3) and also for the $\text{Pr}_{0.7}\text{Ca}_{0.3}\text{CoO}_3$ -derived systems with analogous M-I transition. In important distinction to these previous reports, the transition in present samples $(\text{Pr}_{1-y}\text{Y}_y)_{0.7}\text{Ca}_{0.3}\text{CoO}_3$ exhibits very small thermal hysteresis, which is about 0.2 K for both $y=0.075$ and 0.15. Another

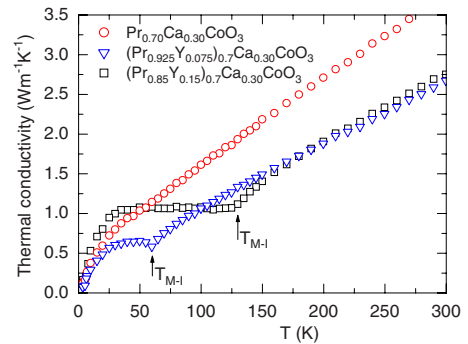


FIG. 3. (Color online) Thermal conductivity of $(\text{Pr}_{1-y}\text{Y}_y)_{0.7}\text{Ca}_{0.3}\text{CoO}_3$ for $y=0, 0.075$, and 0.15 .

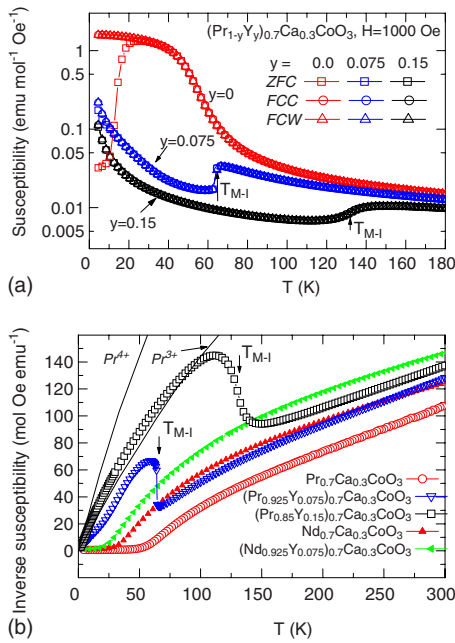


FIG. 4. (Color online) Magnetic susceptibility of (Pr_{1-y}Y_y)_{0.7}Ca_{0.3}CoO₃ for y=0, 0.075 and 0.15 (in log scale). The lower panel shows the temperature dependence of inverse susceptibility. The solid lines mark the theoretical contribution for Pr³⁺ and Pr⁴⁺ ions, calculated for the praseodymium amount in y=0.15 using the data in Ref. 12 (see the text). The data for (Nd_{1-y}Y_y)_{0.7}Ca_{0.3}CoO₃ for y=0 and 0.075 without M-I transition are added for comparison.

property deserving attention is practical absence of residual metallic phase in the insulating ground state, especially for y=0.15. As seen in the plot of inverse susceptibility in lower panel of Fig. 4, the metallic sample Pr_{0.7}Ca_{0.3}CoO₃ undergoes FM-like transition at $T_C \sim 55$ K and, consistently, the magnetization data taken at low temperatures show nearly rectangular hysteresis loops with large coercivity (Fig. 6). On the other hand, the sample y=0.15 exhibits essentially paramagnetic behavior of inverse susceptibility and magnetization curves are of Brillouin type, though some very weak coercivity and remanence appear at 2 K.

The very low susceptibility below T_{M-I} makes sample y=0.15 suitable for a more quantitative analysis. The observed values are obviously smaller than the calculated contribution

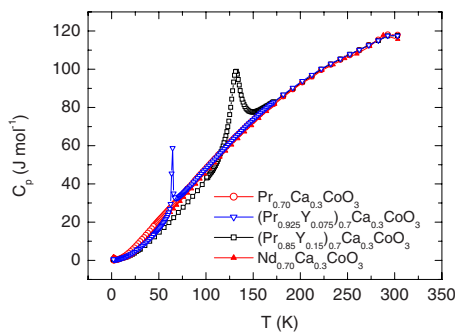


FIG. 5. (Color online) Specific heat of (Pr_{1-y}Y_y)_{0.7}Ca_{0.3}CoO₃ for y=0, 0.075, and 0.15. The data for Nd_{0.7}Ca_{0.3}CoO₃ are added for comparison.

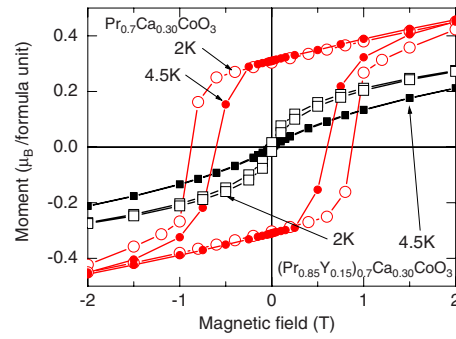


FIG. 6. (Color online) Magnetization loops measured at 2 K (open symbols) and 4.5 K (solid symbols) on (Pr_{1-y}Y_y)_{0.7}Ca_{0.3}CoO₃ (y=0 and 0.15).

of praseodymium ions in trivalent state (see data of Ref. 12 in lower panel of present Fig. 4), disregarding that there should also be contribution of the LS Co⁴⁺ spins. A plausible interpretation provides the new model of M-I transition stating that some praseodymium ions are changed to tetravalent states with lower magnetic moments, and corresponding number of LS Co⁴⁺ ions are transformed to diamagnetic LS Co³⁺. The actual valence shift can be inferred from the thermopower data in Fig. 2. Namely, the thermopower in mixed-valence cobaltites is primarily determined by number of carriers, i.e., by the formal cobalt valence, and, in a less extent, by the average ionic size of large cations in perovskite A sites. Having this in mind, we refer to the fact that Seebeck coefficient in the metallic phase of yttrium doped sample y=0.15

($T \sim 150-300$ K) matches well to Nd_{0.7}Ca_{0.3}CoO₃ with comparable A-site size. This means that cobalt valence in these two samples is practically the same and, consequently, praseodymium ions are essentially in trivalent state, similarly to neodymium ones. Below $T_{M-I}=132$ K, Seebeck coefficient is enhanced and, on further cooling, it becomes comparable to samples with much lower number of carriers, in particular, to Pr_{0.9}Ca_{0.1}CoO₃.¹³ In a rough estimate, this may mean that the formal cobalt valence in y=0.15 is changed upon the M-I transition from original Co^{3.3+} to about Co^{3.1+}.

B. Low-temperature specific heat

At the lowest temperatures, the insulating y=0.075 and 0.15 samples exhibit a steep increase in specific heat (see the c_p/T vs T^2 plot in Fig. 7). Though a similar effect was reported originally for Pr_{0.5}Ca_{0.5}CoO₃ the present experiments, performed down to 0.4 K, document for the first time that the increase is due to Schottky peak, centered at $T=1-2$ K, that adds to common lattice, electronic and nuclear contributions of low-temperature specific heat (Fig. 8). With increasing external field the peak position shifts rapidly to higher temperatures. The Schottky peak is absent in metallic Pr_{0.7}Ca_{0.3}CoO₃ but is found with even larger intensity in Nd_{0.7}Ca_{0.3}CoO₃ with analogous metallic ground state (see Figs. 7 and 9).

The occurrence of Schottky peak in Nd_{0.7}Ca_{0.3}CoO₃ can be understood considering the Kramers character of the rare earth ions. In the orthoperovskite structure, the ⁴I_{9/2} multiplet

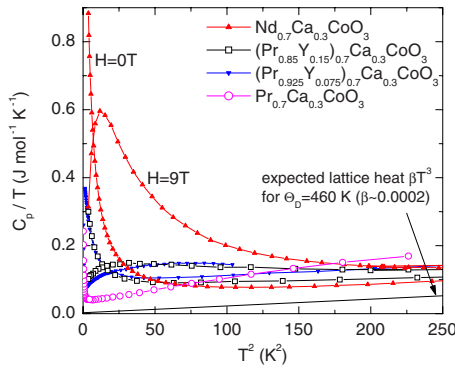


FIG. 7. (Color online) The low-temperature specific heat of $(\text{Pr}_{1-y}\text{Y}_y)_{0.7}\text{Ca}_{0.3}\text{CoO}_3$ and $\text{Nd}_{0.7}\text{Ca}_{0.3}\text{CoO}_3$ shown in the c_p/T vs T^2 plot. Beside common cubic lattice term βT^3 and linear γT term, one may notice an additional contribution for $y=0$, associated with excitations within the crystal-field split multiplet of Pr^{3+} , and an important Schottky anomaly for $y=0.075, 0.15$ and $\text{Nd}_{0.7}\text{Ca}_{0.3}\text{CoO}_3$ that shifts with external field.

of Nd^{3+} is split by crystal-field effects into five relatively distant doublets.¹⁴ The double degeneracy is lifted by an exchange field arising due to FM ordering of cobalt spins. Hence, the Schottky peak under discussion is related to thermal excitations within the ground-state doublet, the location of the maximum defines the energy splitting due to exchange field ($\Delta=0.42k_B T_{max}$) and its shift with applied field bears information on the effective gyromagnetic g_J value that governs the Zeeman splitting ($\Delta=g_J J' \mu_B (B+B_m)$, where $J'=\pm 1/2$ denotes two pseudospin levels of the Kramers doublet and B_m is molecular field acting on the rare-earth moment). The shape of observed Schottky peak is nearly ideal with only a little extra broadening, and the integration of $c_{Schottky}/T$ over T gives the total change in entropy of $3.95 \text{ J K}^{-1} \text{ mol}^{-1}$, in good agreement with the theoretical value $0.7 \text{ N } k_B \ln 2=4.04 \text{ J K}^{-1} \text{ mol}^{-1}$ for $\text{Nd}_{0.7}\text{Ca}_{0.3}\text{CoO}_3$ composition.

In the case of $\text{Pr}_{0.7}\text{Ca}_{0.3}\text{CoO}_3$ the $^3\text{H}_4$ multiplet of Pr^{3+} is split into nine singlets.¹⁵ In accordance with the nonmagnetic (singlet) ground state, there is no Schottky peak at very low temperatures but another Schottky-type contribution emerges at $T>10 \text{ K}$, as can be seen by increased specific heat of

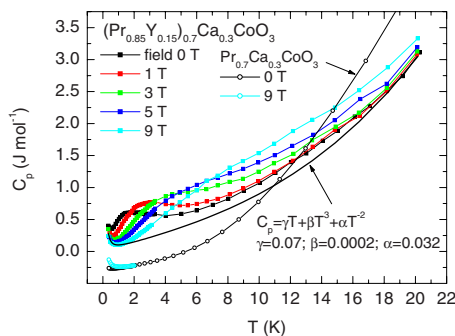


FIG. 8. (Color online) Specific heat of $(\text{Pr}_{1-y}\text{Y}_y)_{0.7}\text{Ca}_{0.3}\text{CoO}_3$ ($y=0.15$) down to 0.4 K , measured in fields $0-9 \text{ T}$. The heat capacity for metallic $\text{Pr}_{0.7}\text{Ca}_{0.3}\text{CoO}_3$ ($y=0$) added for comparison is displaced to -0.3 .

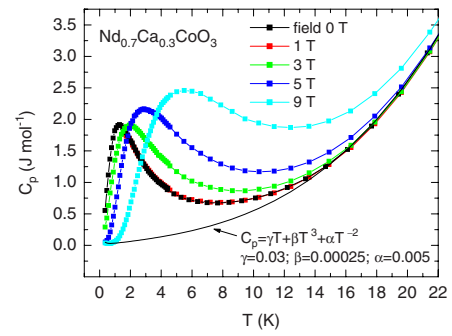


FIG. 9. (Color online) Specific heat of $\text{Nd}_{0.7}\text{Ca}_{0.3}\text{CoO}_3$ down to 0.4 K , measured in fields $0-9 \text{ T}$.

$\text{Pr}_{0.7}\text{Ca}_{0.3}\text{CoO}_3$ in Figs. 7 and 8. It originates in an excitation to the next singlet state at an energy difference of 5 meV .

Analogously to $\text{Nd}_{0.7}\text{Ca}_{0.3}\text{CoO}_3$ the Schottky peak in the yttrium-doped samples $(\text{Pr}_{1-y}\text{Y}_y)_{0.7}\text{Ca}_{0.3}\text{CoO}_3$ can be related to the presence of Kramers ions, which are Pr^{4+} states formed presumably below T_{M-1} . A splitting of the $^2\text{F}_{5/2}$ multiplet to three doublets with large spacing is anticipated. The total entropy change is determined from data in Fig. 8 to $0.98 \text{ J K}^{-1} \text{ mol}^{-1}$ for $y=0.15$. This quantitative analysis enables to estimate the number of Pr^{4+} states to about 0.18 per formula. For $y=0.075$, the entropy change makes $0.61 \text{ J K}^{-1} \text{ mol}^{-1}$ and corresponding number of Pr^{4+} states is 0.12 per formula.

The change in Zeeman splitting of the ground-state doublets with external field is presented in Fig. 10. There is a little shift of $T_{max}(Schottky)$ for $\text{Nd}_{0.7}\text{Ca}_{0.3}\text{CoO}_3$ between zero field and 3 T , before it starts to rise nearly linearly. This shows that the external field does not simply add to the molecular field, in other words, there must be antiparallel or perpendicular orientation of the Nd^{3+} moments with respect to the FM polarized Co spins in the ground state. On the other hand, the shift with external field in the $y=0.15$ sample $(\text{Pr}_{1-y}\text{Y}_y)_{0.7}\text{Ca}_{0.3}\text{CoO}_3$ is monotonous from the very beginning, which is indicative of a parallel orientation of the Pr^{4+} and Co moments.

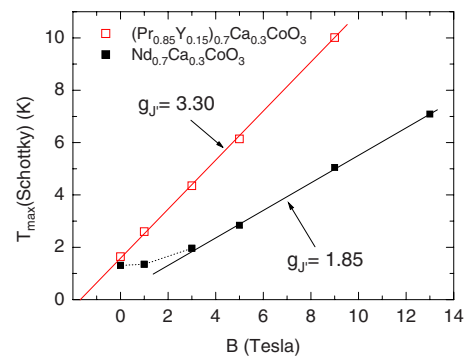


FIG. 10. (Color online) The shift of the Schottky peak maximum (T_{max} in the $c_{Schottky}$ vs T dependence) with applied field. The lines define the effective g factors of the Kramers ground-state doublets of Pr^{4+} and Nd^{3+} . The molecular field experienced by rare-earth moments at $B=0$ is determined to $\sim 1.6 \text{ T}$ in $(\text{Pr}_{1-y}\text{Y}_y)_{0.7}\text{Ca}_{0.3}\text{CoO}_3$ ($y=0.15$) and $\sim 2.5 \text{ T}$ in $\text{Nd}_{0.7}\text{Ca}_{0.3}\text{CoO}_3$.

IV. DISCUSSION

As established in earlier works, the M-I transition in heavily doped cobaltites, such as Pr_{0.5}Ca_{0.5}CoO₃ or (Pr_{1-y}Y_y)_{0.7}Ca_{0.3}CoO₃ is conditioned by presence of praseodymium ions, combined with a suitable structural distortion which depends on an average ionic radius and size mismatch of the perovskite A-site ions (see Ref. 6 and references therein). Important finding of the recent generalized gradient approximation plus *U* electronic-structure calculations for Pr_{0.5}Ca_{0.5}CoO₃ is the location of the occupied Pr³⁺ 4*f* states closely below *E_F* at ambient temperature, and their splitting and partial transfer above *E_F* due to lattice contraction experimentally observed at *T_{M-I}*=90 K. In ionic picture, this means that praseodymium valence in the metallic phase is Pr³⁺, and Pr⁴⁺ valence states are formed in the low-temperature insulating phase, compensated by a valence shift of cobalt ions toward pure Co³⁺. Such scenario is currently supported using different experiments on (Pr_{1-y}Y_y)_{0.7}Ca_{0.3}CoO₃, namely, the low-temperature specific heat, thermopower, and magnetic susceptibility. In addition, some new information on physical properties over a broad temperature range is obtained and deserves more discussion.

The first issue is the character of electronic transport. The data in Fig. 1 suggest that the resistivity in pure Pr_{0.7}Ca_{0.3}CoO₃ tends to a finite value. The metallicity is thus evident despite of the granular character of the ceramic sample. On the other hand, the *y*=0.15 sample of (Pr_{1-y}Y_y)_{0.7}Ca_{0.3}CoO₃ shows a clear localization that is best fitted by Mott's formula for variable range hopping (VRH), $\rho = \rho_o \exp(T_o/T)^{1/4}$, valid for *T* < 40 K [see Fig. 1(b)]. The characteristic parameters are $\rho_o \sim 4 \times 10^{-5}$ mΩ cm and *T_o* ~ 8 × 10⁶ K. The VRH mechanism is associated with a phonon-assisted tunneling of electrons from initial sites located near *E_F* to target sites close in energy, for which the Miller-Abrahams transfer rate applies (see, e.g., recent review of Tessler *et al.*¹⁶). This type of conduction is generally manifested with a specific *T*^{-1/2} dependence of thermopower, which is, however, not obeyed for present samples. Instead, the Seebeck coefficient increases steeply from zero value at the lowest temperatures in a linear metalliclike manner and then tends to a saturation, which is not reached completely because of ingoing transition. Such behavior is suggesting that first, the present system possesses a quasicontinuous, very narrow band of electronic levels at *E_F*, and second, the Seebeck coefficient is related to the presence of carriers rather than to their motion, i.e., the dominant contribution is the change in the net entropy of a solid upon the addition of a charge carrier while the energy transported by carriers, divided by the absolute temperature, seems to be marginal—see, e.g., Ref. 17.

Major experimental data refer, however, to specific heat in the *y*=0.075 and 0.15 samples with occurrence of the M-I transition, compared to samples Pr_{0.7}Ca_{0.3}CoO₃ and Nd_{0.7}Ca_{0.3}CoO₃ with metallic ground state (Figs. 5 and 7). The dominant contribution to the specific heat above the liquid helium temperature is the phononic term that follows in the metallic samples a standard Debye-type dependence, though there is also extra contribution due to thermally activated population of the crystal-field split levels of the

rare earths (see, e.g., Ref. 18). At room temperature the *c_p* value reaches 118 J K⁻¹ mol⁻¹ for all the studied samples. This makes about 93% of the saturated lattice heat taking into account the Dulong-Petit high-temperature limit *c_V*=15 *Nk_B* ~ 125 J K⁻¹ mol⁻¹ in ABO₃ perovskites and a minor correction for thermal expansion *c_p* - *c_V* ~ 1.2 J K⁻¹ mol⁻¹ at 300 K.¹⁸

The phononic term in the low-temperature phase of the yttrium-doped (Pr_{1-y}Y_y)_{0.7}Ca_{0.3}CoO₃ samples is clearly lower than that of the undoped samples. This is a strong indication that M-I transition is accompanied by a significant change in orthoperovskite structure, presumably by the lattice contraction and Pr-O bond length shortening, similar to those in Pr_{0.5}Ca_{0.5}CoO₃.

As concerns the specific-heat anomaly at *T_{M-I}*, the associated entropy change is determined, by integration of an excess of *c_p*/*T*, to 2.17 and 4.78 J K⁻¹ mol⁻¹ for (Pr_{1-y}Y_y)_{0.7}Ca_{0.3}CoO₃ with *y*=0.075 and 0.15, respectively. It is of interest that the total entropy change at the gradual spin-state transitions in *Ln*CoO₃ is about 20 J K⁻¹ mol⁻¹ and is distributed evenly between the first step from the LS Co³⁺ ground state to a LS/HS mixture and the subsequent formation of the metallic phase of IS Co³⁺ character.^{18,19}

At low-enough temperatures, there are two standard contributions of the specific heat, that can be easily distinguished in the *c_p*/*T* vs *T*² plot in Fig. 7. One is the vanishing phononic term, approximated by the cubic term β*T*³ where β is directly related to Debye temperature Θ_{*D*}. The parameters β ~ 0.00020 and 0.00024 J K⁻⁴ mol⁻¹ for the *y*=0.15 sample and Nd_{0.7}Ca_{0.3}CoO₃ shown in the fit in Figs. 8 and 9, give an estimate Θ_{*D*}=460 K and 430 K for the insulating and metallic phase, respectively. The latter value should be compared with Θ_{*D*} ~ 400 K determined for metallic La_{0.7}Sr_{0.3}CoO₃.²⁰ The second contribution is the linear term γ*T*. The γ value ~ 30 mJ K⁻² mol⁻¹ for metallic Pr_{0.7}Ca_{0.3}CoO₃ and Nd_{0.7}Ca_{0.3}CoO₃ is comparable to ~ 40 mJ K⁻² mol⁻¹ for La_{0.7}Sr_{0.3}CoO₃.²⁰ The linear term for the insulating phase of the yttrium-doped samples (Pr_{1-y}Y_y)_{0.7}Ca_{0.3}CoO₃ is significantly larger, γ ~ 70 mJ K⁻² mol⁻¹ for *y*=0.15. Since the enhancement correlates with steeper rise of the low-temperature Seebeck coefficient in Fig. 2, we conclude that the observed linear term is of electronic origin. It arises in consequence of continuous spectrum of density of states, similarly to the electronic heat in metallic conductors but its actual form for essentially localized states in the VRH regime becomes nontrivial because of role of on-site correlations.²¹

The remaining term, as concerns the baseline in Figs. 8 and 9, is the nuclear contribution, manifested as the α*T*⁻² upturn at the lowest temperature. The value α ~ 0.032 mJ K⁻³ mol⁻¹, observed on the *y*=0.15 sample (Pr_{1-y}Y_y)_{0.7}Ca_{0.3}CoO₃ is exceptionally large and apparently field independent. It is worth mentioning that recent specific-heat study on La_{1-x}Sr_xCoO₃ report much smaller nuclear specific heat despite the bulk ferromagnetic state.²⁰ In these compounds, the nuclear heat originates in the Zeeman splitting of the spin *I*=7/2 multiplet of ⁵⁹Co nuclei in the hyperfine field induced by FM ordering of electronic spins. Its intensity thus probes the amount of FM phase in the sample. The very large α*T*⁻² term in the *y*=0.15 sample should be

thus ascribed primarily to contribution of ^{141}Pr nuclei with spin $I=5/2$ in the hyperfine field induced by dressed Pr^{4+} electronic pseudospins. On the other hand, the specific-heat data for pure $\text{Pr}_{0.7}\text{Ca}_{0.3}\text{CoO}_3$ also included in Fig. 8, do not show observable nuclear contribution at zero field but a comparable αT^{-2} term is induced in field of 9 T.

The Schottky peaks observed in $\text{Nd}_{0.7}\text{Ca}_{0.3}\text{CoO}_3$ (Fig. 9) and yttrium-doped $(\text{Pr}_{1-y}\text{Y}_y)_{0.7}\text{Ca}_{0.3}\text{CoO}_3$ (Fig. 8) serve as local probe of the Kramers ions Nd^{3+} and Pr^{4+} . Their position in the zero-field specific heat and shift with applied field allow to estimate that Nd^{3+} pseudospins in $\text{Nd}_{0.7}\text{Ca}_{0.3}\text{CoO}_3$ are characterized by effective $g_{J'}=1.85$ and experience a molecular field of $B_m=2.5$ T while for Pr^{4+} pseudospins in the $y=0.15$ sample $(\text{Pr}_{1-y}\text{Y}_y)_{0.7}\text{Ca}_{0.3}\text{CoO}_3$ the respective values are $g_{J'}=3.30$ and $B_m=1.6$ T (see Fig. 10). The origin of molecular field in metallic $\text{Nd}_{0.7}\text{Ca}_{0.3}\text{CoO}_3$ is in ferromagnetic ordering of cobalt ions in IS states at $T_C\sim 25$ K ($M_s\sim 0.16\mu_B$ per f.u.) and their interaction via $3d-4f$ exchange mechanisms with spin component of the Nd^{3+} moments. The situation in the low-temperature phase of $(\text{Pr}_{1-y}\text{Y}_y)_{0.7}\text{Ca}_{0.3}\text{CoO}_3$ which exhibits essentially paramagnetic characteristics (see Figs. 4 and 6) is not clear and will require further experimental and theoretical investigation. If Pr^{4+} pseudospins were ordered spontaneously, significantly sharper and higher peak (so called lambda peak) would be observed as is, e.g., in the case of antiferromagnetic ordering of Nd^{3+} moments in NdCoO_3 at $T_N=1.2$ K.²² The observation of standard Schottky peak thus suggests that also in the yttrium-doped samples the rare earths experience a stable molecular field induced by the cobalt subsystem. We note that the cobalt subsystem in the $y=0.15$ sample contains 12% of LS Co^{4+} ions that represent spins 1/2 in a diamagnetic matrix of LS Co^{3+} . Anticipating their itinerancy they may lead to certain ferromagnetic polarization of the narrow t_{2g} cobalt bands, low compared to $\text{Nd}_{0.7}\text{Ca}_{0.3}\text{CoO}_3$ but sufficient to mediate relatively strong magnetic interactions among the Pr^{4+} pseudospins (Ruderman-Kittel-Kasuya-Yoshida model known for $3d-4f$ intermetallics can be envisaged²³). Such interpretation seems to be supported by two findings—the parallel orientation of praseodymium moments with cobalt spins, manifested in the field-induced shift of Schottky peak in Fig. 10, and the unusually large term αT^{-2} contributed by the ^{141}Pr nuclear spins, seen for the $y=0.15$ sample $(\text{Pr}_{1-y}\text{Y}_y)_{0.7}\text{Ca}_{0.3}\text{CoO}_3$ in Fig. 8.

V. CONCLUSION

A comparative study of perovskite cobaltites $(\text{Ln}_{1-y}\text{Y}_y)_{0.7}\text{Ca}_{0.3}\text{CoO}_3$ perovskites ($\text{Ln}=\text{Pr},\text{Nd}$) was under-

taken with an aim to elucidate the character of a peculiar first-order M-I transition in some Pr-based cobaltites. Though the transition is typical for $\text{Pr}_{0.5}\text{Ca}_{0.5}\text{CoO}_3$, the present yttrium-doped systems $(\text{Pr}_{1-y}\text{Y}_y)_{0.7}\text{Ca}_{0.3}\text{CoO}_3$ with $T_{M-I}=64$ K and 132 K for $y=0.075$ and 0.15, respectively, appear preferable because of easier stabilization of the stoichiometric phase and complete transformation from the metallic to insulating state. The study shows that the M-I transition is manifested by a huge peak in the specific-heat data and marked changes in the electrical resistivity, thermopower, and thermal conductivity. A sudden drop of magnetic susceptibility indicates a change in cobalt states from the metallic $t_{2g}^5\sigma^*$ to the mixture of LS Co^{3+} (t_{2g}^6) and LS Co^{4+} (t_{2g}^5).

An important novelty is an observation of Schottky peak in specific-heat data at very low temperatures, 0.4–10 K. This peak is absent in pure $\text{Pr}_{0.7}\text{Ca}_{0.3}\text{CoO}_3$ in which metallic phase is retained down to the lowest temperature but appears with large intensity in $\text{Nd}_{0.7}\text{Ca}_{0.3}\text{CoO}_3$ with similar metallic phase. Its occurrence follows from the Kramers character of Nd^{3+} and Pr^{4+} whose $^4I_{9/2}$ and $^2F_{5/2}$ multiplets are split by crystal field associated with the distorted dodecahedral coordination of the rare earths in the $Pbnm$ perovskites. The Schottky peak thus probes the Zeeman splitting of the ground-state doublet. The total entropy change associated with the Schottky peak is $k_B \ln 2$ per ion, which allows to determine the concentration of Kramers ions in the samples experimentally, by integration of c_{Schottky}/T over T . The analysis for the $y=0.075$ and 0.15 samples $(\text{Pr}_{1-y}\text{Y}_y)_{0.7}\text{Ca}_{0.3}\text{CoO}_3$ provides values 0.12 and 0.18 Pr^{4+} per formula unit, respectively. Considering that praseodymium ions are essentially in trivalent state in the high-temperature phase, the observation of Pr^{4+} in the low-temperature phase is in accordance with idea that the simultaneous M-I and spin-state transition in Pr-based cobaltites is accompanied by an electronic transfer between the praseodymium and cobalt ions. In particular, for $y=0.15$, the present results are indicative of a significant change from common valence distribution in the metallic state, $(\text{Pr}_{0.85}^{3+}\text{Y}_{0.15}^{3+})_{0.7}\text{Ca}_{0.3}^{2+}\text{Co}_{0.7}^{3+}\text{Co}_{0.3}^{4+}\text{O}_3^{2-}$, to $(\text{Pr}_{0.59}^{3+}\text{Pr}_{0.26}^{4+}\text{Y}_{0.15}^{3+})_{0.7}\text{Ca}_{0.3}^{2+}\text{Co}_{0.88}^{3+}\text{Co}_{0.12}^{4+}\text{O}_3^{2-}$ in the insulating state.

ACKNOWLEDGMENT

This work was supported by Project No. 202/09/0421 of the Grant Agency of the Czech Republic.

¹Z. Jiráček, J. Hejtmánek, K. Knížek, and M. Veverka, *Phys. Rev. B* **78**, 014432 (2008).

²S. Tsubouchi, T. Kyômen, M. Itoh, P. Ganguly, M. Oguni, Y. Shimojo, Y. Morii, and Y. Ishii, *Phys. Rev. B* **66**, 052418 (2002).

³S. Tsubouchi, T. Kyômen, M. Itoh, and M. Oguni, *Phys. Rev. B* **69**, 144406 (2004).

⁴T. Fujita *et al.*, *J. Phys. Soc. Jpn.* **73**, 1987 (2004).

⁵T. Fujita, S. Kawabata, M. Sato, N. Kurita, M. Hedo, and Y. Uwatoko, *J. Phys. Soc. Jpn.* **74**, 2294 (2005).

⁶T. Naito, H. Sasaki, and H. Fujishiro, *J. Phys. Soc. Jpn.* **79**, 034710 (2010).

⁷K. Knížek, J. Hejtmánek, P. Novák, and Z. Jiráček, *Phys. Rev. B* **81**, 155113 (2010).

- ⁸A. J. Barón-González, C. Frontera, J. L. García-Muñoz, J. Blasco, and C. Ritter, *Phys. Rev. B* **81**, 054427 (2010).
- ⁹J. Wu and C. Leighton, *Phys. Rev. B* **67**, 174408 (2003).
- ¹⁰K. Knížek, Z. Jirák, J. Hejtmánek, and P. Novák, *J. Magn. Magn. Mater.* **322**, 1221 (2010).
- ¹¹J. Hejtmánek, Z. Jirák, M. Maryško, C. Martin, A. Maignan, M. Hervieu, and B. Raveau, *Phys. Rev. B* **60**, 14057 (1999).
- ¹²K. Sekizawa, M. Kitagawa, and Y. Takano, *J. Magn. Magn. Mater.* **177-181**, 541 (1998).
- ¹³H. Masuda, T. Fujita, T. Miyashita, M. Soda, Y. Yasui, Y. Kobayashi, and M. Sato, *J. Phys. Soc. Jpn.* **72**, 873 (2003).
- ¹⁴A. Podlesnyak, S. Rosenkranz, F. Fauth, W. Marti, A. Furrer, A. Mirmelstein, and H. J. Scheel, *J. Phys.: Condens. Matter* **5**, 8973 (1993).
- ¹⁵A. Podlesnyak, S. Rosenkranz, F. Fauth, W. Marti, H. J. Scheel, and A. Furrer, *J. Phys.: Condens. Matter* **6**, 4099 (1994).
- ¹⁶N. Tessler, Y. Preezant, N. Rappaport, and Y. Roichman, *Adv. Mater.* **21**, 2741 (2009).
- ¹⁷D. Emin, in *Thermoelectrics Handbook: Macro to Nano*, edited by D. M. Rowe (CRC Press, London, 2006), Chap. 5.
- ¹⁸K. Knížek, J. Hejtmánek, Z. Jirák, P. Tomeš, P. Henry, and G. André, *Phys. Rev. B* **79**, 134103 (2009).
- ¹⁹M. Tachibana, T. Yoshida, H. Kawaji, T. Atake, and E. Takayama-Muromachi, *Phys. Rev. B* **77**, 094402 (2008).
- ²⁰C. He, S. Eisenberg, C. Jan, H. Zheng, J. F. Mitchell, and C. Leighton, *Phys. Rev. B* **80**, 214411 (2009).
- ²¹The simple relation between electronic heat and density of states in metals derives from Fermi-Dirac statistics that is based on principle of double (spin-up, spin-down) occupancy of electronic levels. At the presence of correlations and preference of single occupancy as in Hubbard model, the electronic heat is significantly modified, see J. Spałek and W. Wójcik, *Phys. Rev. B* **37**, 1532 (1988).
- ²²F. Bartolomé, M. D. Kuz'min, J. Bartolomé, J. Blasco, J. García, and F. Sapiña, *Solid State Commun.* **91**, 177 (1994).
- ²³J. J. M. Franse and R. J. Radwanski, in *Handbook of Magnetic Materials*, edited by K. H. J. Buschow (Elsevier, New York, 1993), Vol. 7, Chap. 5.